16th International Conference on Greenhouse Gas Control Technologies, GHGT-16

23rd -27th October 2022, Lyon, France

A new facility for viscosity and density measurements for CO_2 – rich mixtures relevant for CO_2 transport and storage

Bahareh Khosravi[a], Anders Austegard[b], Hans Georg Jacob Stang[b], Caroline Einen[b], Jana Poplsteinova Jakobsen[a], Ingrid Snustad[b], Sigurd Weidemann Løvseth[b]*

[a]Norwegian University of Science Technology (NTNU), NO-7491, Trondheim, Norway

[b]SINTEF Energy Research, NO-7465 Trondheim, Norway

Abstract

For safe and cost-effective design, optimization, and operation of CO_2 capture, transport, and storage (CCS) processes, accurate viscosity and density data of CO_2-rich mixtures are required. Currently, there are large knowledge gaps in these properties, and it needs to be addressed for building good reservoir models and simulation tools. A modified two-capillary viscometer with several novel solutions for accurate measurement of viscosity and density of CO_2-rich mixtures relevant for CO_2 transport and storage has been designed and constructed. The new setup covers a range between 213.15 K and 423.15 K in temperature and up to 100 MPa in pressure. This paper describes the facility, calibrations, uncertainties estimation, and first test measurements performed using the setup.

Keywords: CO_2 transport and storage; thermophysical properties; CO_2 impurities; viscosity, density

1. Introduction

Costs and perceived risks are major barriers to widespread implementation of CCS [1]. One of the key constraints is the impact of potential impurities being present in the CO_2 streams and also uncertainty of relevant process simulation models [2]. A small amount of impurities can significantly change the thermophysical properties of CO_2-rich mixtures [3, 4]. Accurate, reliable, and consistent experimental data for thermophysical properties are needed in order to optimize the operational conditions and the energy consumption of purification, compression, liquefaction, transport, and storage [5]. There are still important data gaps remaining for CCS, which are crucial for building good reservoir models and simulation tools. Uncertainties in these properties can lead to costly overdesign and/or risks of inefficient or unsafe injection and storage.

Fluid property data on gas and liquid viscosity are necessary to determine pressure drop and heat transfer in CO_2 capture processes, as well as essential design and operational parameters for CCS processes [6, 7]. Flow regime determination, pump/compressor power consumption, the performance of heat exchangers, reservoir injectivity index, plume evolution, storage efficiency, and simulations of laminar reservoir flows are all dependent on viscosity. Viscosity is also necessary to predict convection and diffusion processes, and the sweep efficiency of CO_2 EOR depends strongly on the CO_2/reservoir fluid viscosity ratio. Density is a critical property for almost all processes within CCS and the development of equations of state predicting all other thermodynamic properties.

Data gaps between available and required experimental data ranges for the transport properties of CO_2-rich mixtures have been recognized. For instance, for liquid phase viscosity and relevant compositions, only two somewhat limited data sets from a single lab have been identified [8, 9]. Little data are available for the gas phase. The situation for density is better, but most binary systems still have significant knowledge gaps or limited data. For some data are lacking altogether [10].

This research project aims to reduce CCS cost and risk by acquiring high-quality data on the viscosity and density properties of pure CO_2 and CO_2-rich mixtures with relevant impurities and additives under CO_2 transport and storage conditions. In addition, the new data will improve models for the same fluids and conditions, which will be applied in relevant reservoir simulation tools. Acquiring high-quality data requires a well-characterized experimental apparatus with a well-defined uncertainty level. The apparatus includes a modified two-capillary viscometer [11] with several novel solutions to enable high performance over an extensive range in pressure and temperature. Integrated with the setup is a densimeter controlled to the same temperature and pressure as viscosity for the density measurements. The experiment procedure relies on measuring the pressure drop through capillaries which is proportional to both the flow and the viscosity of laminar flow. The setup covers temperatures between 213.15 K and 423.15 K in temperature and pressures up to 100 MPa for pure, liquid, supercritical, or gaseous states. This work will summarize a brief description of the setup, calibration system, routines, and initial validation data.

2. Principle of measurement

The theory of the capillary viscometers is based on Hagen–Poiseuille equation [12]. For a compressible and Newtonian fluid in laminar flow through at locations z along a tube capillary, can write the following equation:

$$\int_{P_1,T}^{P_2,T} \frac{\rho_m(T,P)}{\eta(T,P)} dP = \int_0^L -\frac{8\dot{n}}{\pi r^4} dz \tag{1}$$

Here dP is the pressure drop, P_1 and P_2 are pressures at inlet and outlet of the capillary, respectively, η is the dynamic viscosity of the fluid at the temperature of T, r is the inner diameter of the capillary, L is the capillary length, $\dot{n}$ is molar flow rate, and ρ_m is the molar density.

The principle of experiments is based on measuring pressure drop along a capillary tube. Two-capillary viscometer works somewhat; the upstream capillary is at test pressure and temperature *(T, P)*, and the downstream reference capillary operates at a constant low pressure of around 0.1 MPa and reference temperature of 298.15 K. The pressure drop across the upstream capillary is proportional to the viscosity at the test temperature and pressure, while the pressure drops over the upstream capillary at reference conditions (298.15 K and 0.1 MPa) is proportional to the mass flow. The idea beyond this is that the flow rate through both capillaries is identical. Therefore, keeping the flow rate constant through upstream and downstream capillaries is essential, so that the mass flow can be gravimetrically calibrated at downstream.

For accurate measurements, the ratio viscosity measurements approach is, where the known very accurate viscosity of helium at reference conditions is used as a reference [13]. In order to cancel out the capillary geometry effects, measurements for helium must be carried out just after or before the test gas. The following working equation can be defined to estimate the viscosity of the test fluid:

$$\eta_{P,T}^{fld} = \left(\eta_{0,298}^{He}\right)_{abinitio} \left(\frac{\eta_{0,T}^{He}}{\eta_{0,298}^{He}}\right)_{abinitio} \left(\frac{\eta_{P,T}^{He}}{\eta_{0,T}^{He}}\right) \left(\frac{\eta_{0,298}^{fld}}{\eta_{0,298}^{He}}\right) \left(R_{T,298}^{fld}\right)_{P,0} \tag{2}$$

This equation includes five factors:

1) $\left(\eta_{0,298}^{He}\right)_{abinitio}$: viscosity of helium at zero density and 298.15 K which is calculated with an *ab initio* [14] method from quantum mechanics and statistical mechanics, with uncertainty less than 0.01 %.
2) $\left(\eta_{0,T}^{He} / \eta_{0,298}^{He}\right)_{abinitio}$: the temperature-dependent ratio for the viscosity of helium at 298.15 K and desired temperature *T* which is calculated *ab initio* [14] with uncertainty less than 0.01 % in the range 200 K < *T* < 400 K.
3) $\left(\eta_{P,T}^{He} / \eta_{0,T}^{He}\right)$: the temperature-dependent ratio for helium viscosity at desired pressure *P* and the zero density. This could be obtained with the two-capillary viscometer by setting both baths at temperature *T* and operating the upstream capillary first at low pressure and then at high pressure *P*.
4) $\left(\eta_{0,298}^{fld} / \eta_{0,298}^{He}\right)$: a reference value for the viscosity ratio, measured at 298.15 K for both helium and test fluid.
5) $\left(R_{T,298}^{fld}\right)_{P,0}$: measurement of the temperature-dependent ratio of viscosity ratios which is determined from:

$$\left(R_{T,298}^{fld}\right)_{P,0} = \left(\frac{\eta_{P,T}^{fld}}{\eta_{0,298}^{fld}}\right) / \left(\frac{\eta_{P,T}^{He}}{\eta_{0,298}^{He}}\right) \tag{3}$$

$\left(R_{T,298}^{fld}\right)_{P,0}$ could be substituted with below equation even where the ideal gas law is no longer applicable.

$$\left(R_{T,298}^{fld}\right)_{P,0} = \frac{\left(P_3^2 - P_4^2\right)^{He}\left[\left(\rho_1 + \rho_2\right).\left(P_1 - P_2\right)\right]^{fld}.C^{*fld}\left(T, P_1, P_2\right)C^{He}\left(298.15K, P_3, P_4\right)}{\left(P_1^2 - P_2^2\right)^{He}\left[\left(\rho_3 + \rho_4\right).\left(P_3 - P_4\right)\right]^{fld}.C^{*He}\left(T, P_1, P_2\right)C^{fld}\left(298.15K, P_3, P_4\right)} \tag{4}$$

An accurate hydrodynamic model for fluids through a capillary can be implemented by considering proper correction factors *C* and *C**, as presented by Ref. [13, 15]. These parameters correct the initial assumptions of model: 1) departures from ideal gas accounted for both density and viscosity virial coefficients, 2) slip at the capillary wall, 3) kinetic energy changes at the capillary entrance, 4) gas expansion along the length of the capillary due to the pressure drop, 5) thermal distribution along the capillary and 6) centrifugal effect due to the coil capillaries.

3. Experimental Infrastructure

A simple schematic diagram and a photograph of the installed experimental infrastructure are shown in Fig. 1 and Fig. 2. A detailed description of the new facility with an experimental procedure is reported in a previous publication [16] and only a brief overview will be presented here. Helium, CO_2, or prepared CO_2-rich mixtures flow through the tubing from the gas supply into a syringe pump, where the fluid is injected into the upstream capillary at the desired pressure. The pump is connected to a buffer volume for faster pressurization as well as stabilization of the upstream pressure. Then the fluid flows through the upstream capillary at the desired pressure and temeprature. The pump is also connected to the densimeter, enabling density measurement at the condition as viscosity. For temperature control,

the capillaries are immersed in the thermostatic containers in a horizontal orientation. The thermostatic containers with capillaries are placed inside large containers which are vacuum insulated to decrease heat loss to the surroundings and facilitate high-temperature uniformity. For this purpose, a vacuum pump (including a pre-vacuum pump and a turbomolecular pump for high vacuum pressure) is used. In order to measure the temperature and thermal uniformity, two 25Ω Standard PRTs (SPRTs) and several platinum resistance thermometers (PRTs) are mounted.

The pressure drop is determined by measuring the pressure at the input and output of the capillaries with an array of very precise pressure transmitters. During a measurement, the pressures P_1, P_3, and P_4 are controlled using three impedances: the high-pressure syringe pump, pressure reduction system, and a leak valve, respectively. The measurement of P_2 is needed to estimate the viscosity and the pressure drops (P_1-P_2) across the upstream capillary. In order to improve the precision of pressure drops measurements, the bias between inlet and outlet pressure transmitters must be measured before and after each measurement point. The pressure reduction system includes a cascade system of six shut-off valves, five capillary coils, and a control valve to decrease the target pressure P at upstream to reference pressure (average of P_3, and P_4) around 0.1 MPa at downstream.

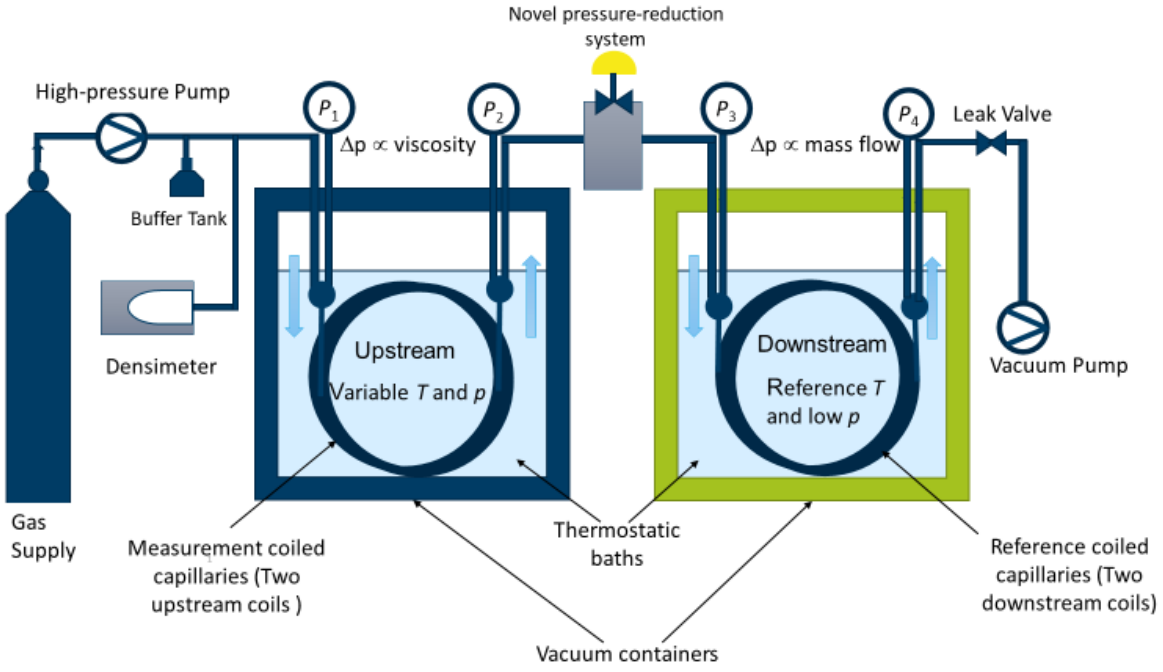

Fig. 1: A simplified schematic of two- capillary viscometer.

Fig. 2: A picture of two- capillary viscometer facility.

4. Uncertainty analysis

The overall combined standard uncertainty for the viscosity measurements *uc (η (T, P, x))* will be conducted from:

$$u_c(\eta(T,P,x)) = \sqrt{u(\eta)^2 + [(\partial\eta/\partial T)_{(p,x)}u(T)]^2 + [(\partial\eta/\partial P)_{(T,x)}u(P)]^2 + [(\partial\eta/\partial x)_{(P,T)}u(x)]^2} \quad (5)$$

where *u(η)*, *u(T)*, *u(p)*, and *u(x)* are the standard uncertainties of the viscosity, temperature, pressure, and composition in the case of mixtures, respectively. The temperature uncertainty was determined from the temperature calibration based on the temperature calibration standard ITS-90 (International Temperature Scale of 1990 [18]), as discussed in section 5.1. Moreover, temperature uniformity and stability during main measurements will be considered as additional sources of temperature uncertainty. To check the temperature uniformity of the upstream capillary, where the viscosity is measured, a SPRT and a PT100 sensors are mounted at the bottom of the thermostatic container and two PT00 at the top. Temperature stability of ±10 mK will be achieved during the viscosity measurements. Pressure calibration is needed to quantify the pressure uncertainty. Section 5.2 will describe the pressure calibration procedure performed for all the pressure sensors. CO_2- rich mixtures with an accuracy desired are not commercially available. Therefore, an in-house setup [17] will be used to prepare calibration gas mixtures gravimetrically. There will also be a composition check by a Gas Chromatograph (GC) available in the lab. The main contribution to the expanded combined uncertainty is the uncertainty from the viscosity measurements *u(η)*. The viscosity of helium calculated *ab*

initio [14] with a small uncertainty is used to calibrate two-capillary viscometers by cancelling out the geometry effects of capillaries. The main uncertainty of viscosity will be dominated by pressure drops across the capillaries, mass flow measurements, and reproducibility of the viscometer. In order to improve the precision of pressure drops measurements, the bias between inlet and outlet pressure transmitters was measured just before and after each measurement point. The mass flow measurements and reproducibility of the viscometer will be discussed in Sections5.2, and 5.3, respectively.

5. Calibration

5.1. Temperature calibration:

In total six temperature sensors, including two 25 Ω standard platinum resistance thermometers (SPRT) and four 100 Ω PT100s, are installed for temperature control and measurements. All sensors were calibrated according to the temperature calibration standard ITS-90 (International Temperature Scale of 1990 [18]). Because SPRTs have higher accuracies than PT100s, it is recommended to use fixed-point cells for calibration purpose. However, PT100s have more significant uncertainties, so a comparative calibration method against a reference SPRT is common. As the operating temperature for viscosity measurements is in the range of 213.15 K to 423.15 K, the ITS-90 framework using fixed points was performed in three subranges: the freezing point of Indium (T90 ≡ 429.7485 K), the melting point of gallium (T90 ≡ 302.9146 K), the triple point of water (T90 ≡ 273.16 K) and the triple point of mercury (T90 ≡ 234.3156 K). As seen from Fig. 3, the maximum deviation is -86.75 mK, corresponding to the freezing point of Indium for SPRT #1. A linear fit was used for the temperature calibration, where the maximum deviation is less than 20 mK for SPRT #2 from the melting point of gallium. This deviation still allows measurements to meet the desired combined viscosity uncertainty of 0.1%. For temperatures out of the calibration range, below 234.31 K and higher than 429.74 K, an extrapolation using is necessary.

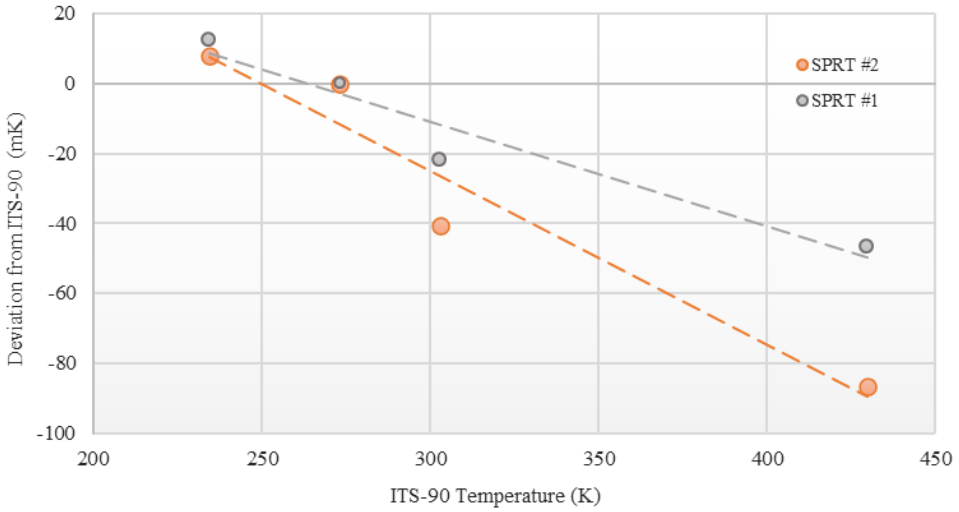

Fig. 3: Temperature deviation of SPRTs from the ITS-90 fixed points as a function of ITS-90 temperature. Data points show the temperature deviation of SPRTs (calibration results) at the freezing point of Indium (T90 ≡ 429.7485 K), the melting point of gallium (T90 ≡ 302.9146 K), the triple point of water (T90 ≡ 273.16 K) and the triple point of mercury (T90 ≡ 234.3156 K). The dashed line corresponds to a linear fit.

The comparative calibration of four PT100 sensors was carried out against two SPRTs, and an average temperature was used as the reference temperature. All sensors were mounted in an Aluminum block placed inside a thermostatic bath. Copper oxide powder was used to increase thermal conductivity. The calibration was performed at 15 points to cover the operating range between 213.15 K and 423.15 K. An example of comparative calibration is shown in Fig. 4. The calibration results show a good agreement with the data obtained by factory.

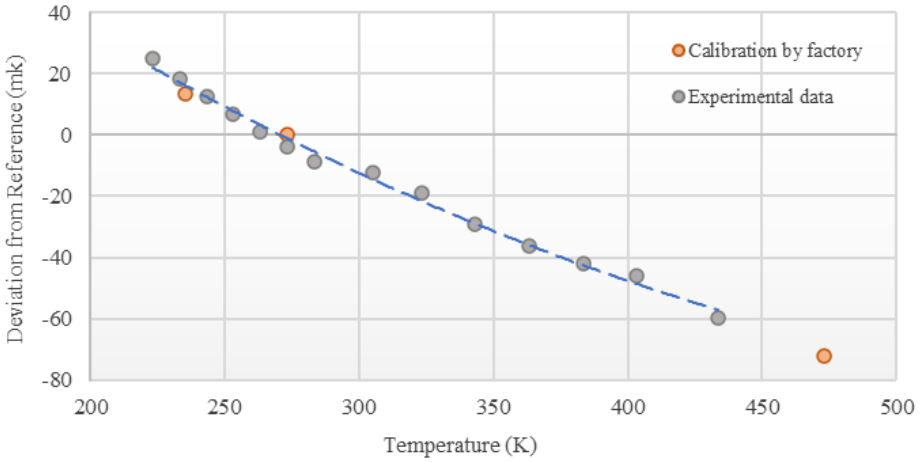

Fig. 4: Temperature deviation of PT10 (#5) from the average temperature of reference SPRTs. Color marks show the calibration results from factory. Grey marks show the calibration data within this work. The dashed line corresponds to a second-order polynomial fit.

5.2. Pressure Calibration

Since the pressure drop is proportional to the viscosity of laminar flow, high accuracy of pressure measurements is crucial, and also, the pressure must stabilize to high relative precision. Therefore, an array of custom-made precision pressure transmitters with different full-scale pressures of 2.1, 6.9 and 13.8 MPa (Paroscientific), and 100 MPa (Keller) are used.

All pressure sensors were calibrated in-house against a dead weight, where three different piston cells with different pressure range and uncertainty were used; cell_10: up to 1 MPa and accuracy 0.00002 MPa + 0.01%, cell_50: up to 5 MPa and accuracy 0.0001 MPa + 0.01% and cell_200: up to 20 MPa and accuracy 0.0004 MPa + 0.01%. The high-pressure syringe pump was used to control the target pressure during the calibration. The pressure reading from calibration is defined as gauge pressure and the atmospheric pressure and hydrostatic pressure need to be considered

$$P_{\mathrm{Re}\,f} = P_{reading} + P_{atm} + P_{hydrostatic} \tag{6}$$

Where $P_{reading}$ is determined from the calibration, P_{atm} is the local atmospheric pressure and $P_{hydrostatic}$ is the hydrostatic pressure due to level difference between pressure sensors and deadweight (around 0.55 m high).

The result graphs are complex and numerous, but to sum up, the maximum pressure (P_{max}) where the uncertainty terms included have a contribution lower than Max. Error are summed up in the table below:

Table 1. Results for the pressure uncertainty

P_{max} (MPa)	Max. Error (%)
2.5	0.05
6.5	0.1
12.5	0.2
43	0.5
100	1

5.3. Mass flow calibration

Besides the pressure and pressure drop measurements to calculate the viscosity, the mass flow of fluid must be known. For this purpose, the reference capillary combined with a custom-made gravimetric setup act as a flow meter. For this purpose, both helium and fluid under test alternatively flow through the downstream capillary from a sphere filled with the fluid in advance. The sphere's mass with content must be weighed before starting flow measurement. During the flow measurement, the reference temperature 298.15 K and pressures P_3 and P_4 at predetermined values keep constant during the flow period. Hence, the unknown flow rate of the helium or fluid under test that has flowed through the downstream capillary is constant as well. Then, the $\dot{m}$ which is calibrated gravimetrically can be very accurately determined by:

$$\dot{n} = M\dot{m}, \tag{7}$$

$$\dot{m} = \frac{m_{sphere}^{before} - m_{sphere}^{after}}{t}. \tag{8}$$

m_{sphere}^{before} and after m_{sphere}^{after} are the sphere's mass with content before and after the flow measurement. M and t are the fluid mass molar and the flow period, respectively. An optimum flow must be determined to meet the high accuracy of measurements as well as keep the flow in the laminar flow region. Pressures P_3 and P_4 were set at predetermined values of 0.115 MPa and 0.085 MPa, respectively. The experiments were performed for helium and CO_2, and the final results can be found in the table below.

Table 2. Mass flow calibration results for helium and CO_2.

Fluid	Number of experiments	Duration (h)	Average mass flow (µg /s)	Repeatability (%)
He	3	14.72	41.9949	0.25
CO_2	3	10.09	615.5525	0.02

The leakage investigation shows a leakage of 0.0027 (µg /s) and considered in the mass flow calculation. The mass flow reportability of CO_2 is smaller than the one of helium at the condition mainly due to higher molecular weight of CO_2.

6. Initial tests

Test operation for helium has been recently conducted to check the reproducibility of the two-capillary viscometer. Initial tests were measured at two isotherms, 278.15 K and 313.15 K since it was easier to work with water as a thermostat fluid in the first attempts. In order to make the experiment time effective, the measurements were performed isotherm per isotherm. First, the thermostatic system was filled with water. Then the upstream capillary's set-point temperature was set at the measurement temperature *T*, and the downstream capillary's set-point was the reference temperature 298.15 K. It is required to ensure that the temperature of both upstream and downstream capillaries is fully stabilized before starting the main measurements. So, the temperatures were set a night before. Then, helium flowed through the upstream capillary with an inner diameter of 200 μm and a length of 11.671 m, followed by the downstream capillary with an inner diameter of 500 μm and 8.563 m in length. During the measurement, P_1 was controlled by the high-pressure syringe pump at the desired pressure 3 MPa, the pressure reduction system regulated P_3 at a pressure of 0.115 MPa and P_4 was controlled at a pressure of 0.085 MPa using the leak valve at the end of the system. The pressure drops (P_3-P_4) of 0.03 MPa is corresponding the mass flow of helium reported in Table 2. The P_2 was measured to estimate the pressure drops (P_1-P_2) across the upstream capillary.
To quantify the reproducibility of the viscometer, 4 tests at 278.15 K and 4 tests at 313.15 K for a pressure of 3 MPa were repeated and a reproducibility of 0.04% and 0.13% were achieved, respectively.

Table 3. The reproducibility of the viscometer at almost T= 278.15 K and *P*= 3 MPa, where ΔP_{12} is the pressure drop across upstream capillary and ΔP_{34} is the pressure drop across downstream capillary

Test No.	T (K)	ΔP_{12} (MPa)	ΔP_{34} (MPa)	ΔP_{12} /ΔP_{34}
1	278.15	0.0478	0.0300	1.5941
2	278.15	0.0478	0.0300	1.5937
3	278.17	0.0478	0.0300	1.5926
4	278.17	0.0478	0.0300	1.5931
		Std. / MPa		0.001
		Error %		0.04%

Table 4. The reproducibility of the viscometer at almost T= 313.15 K and *P*= 3 MPa, where ΔP_{12} is the pressure drop across upstream capillary and ΔP_{34} is the pressure drop across downstream capillary

Test No.	T (K)	ΔP_{12} (MPa)	ΔP_{34} (MPa)	ΔP_{12} /ΔP_{34}
1	313.111	0.0585	0.0300	1.9502
2	313.109	0.0585	0.0300	1.9472
3	313.124	0.0585	0.0300	1.9491
4	313.151	0.0584	0.0300	1.9440
		Std. / MPa		0.003
		Error %		0.14%

Fig. 5 shows the pressure drop across upstream (blue) and downstream (red) capillaries of a data point (*T*=313.15 K, *P*=3 MPa) as an example. Each measurement should start and end with the bias measurements for the pressure sensor used. A duration of at least 5 minutes (Elapsed time: 0-12 min and 80-90 min) were considered. The main measurement must be taken when the pressure drops across upstream and downstream capillaries are constant for at least 20 minutes. In this case, the pressure drops are constant between the elapsed time of 32 and 70 minutes with a standard deviation

of 99.2 Pa and 12.7 Pa for pressure drops (P_1-P_2) and (P_3-P_4), respectively. The operation of processes was carried through by the LabVIEW control and data acquisition program.

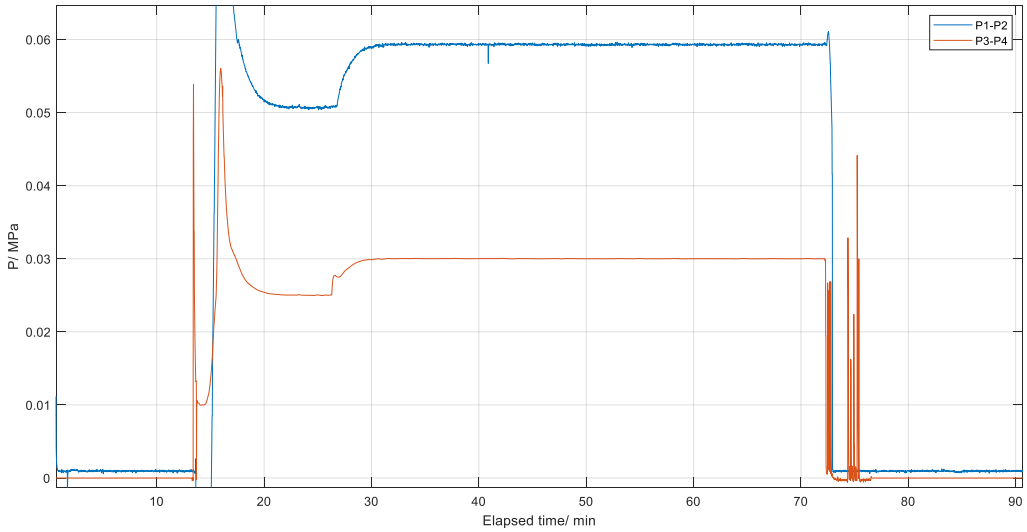

Fig. 5: An example of the pressure drops across upstream (blue) and downstream (red) capillaries of a data point (T=313.15 K, P=3 MPa) during the measurement.

7. Conclusions and next steps

A two-capillary viscometer has been designed and built for measurements of viscosity and density of CO_2-rich mixtures relevant for CO_2 transport and storage. The setup aims for high accuracy data for pressures up to 100 MPa and temperatures between 213.15 K and 423.15 K. To meet the high target uncertainty, a great accuracy in pressure, temperature, flow, and composition in case of the mixture is required. Sophisticated calibration procedures and routines were followed to minimize and quantify the uncertainty of measurements. In addition, the initial tests for the characterization of the setup were performed. In the next step, the correction factors need to be implemented into the hydrodynamic model and improve the accuracy of experimental data. Furthermore, validation data for pure CO_2 and mixtures through the whole range of temperature and pressure will be measured. The next plan is to measure new experimental data for binary CO_2- rich mixtures, where there is a high demand to develop thermophysical models relevant for CO_2 transport and storage.

Acknowledgements

This publication has been produced with support from the from the research program CLIMIT and the NCCS Centre, performed under the Norwegian research program Centres for Environment-friendly Energy Research (FME). The authors acknowledge the following partners for their contributions: Aker Solutions, ANSALDO Energia, CoorsTek Membrane Sciences, EMGS, Equinor, Gassco, KROHNE, Larvik Shipping, Lundin, Norcem, Norwegian Oil and Gas, Quad Geometrics, TOTAL, and the Research Council of Norway (257579/E20 and 280394).

References

[1] E. S. Rubin, J. E. Davison, and H. J. Herzog, "The cost of CO2 capture and storage," *International Journal of Greenhouse Gas Control*, vol. 40, pp. 378-400, 2015.

[2] C. Eickhoff *et al.*, "IMPACTS: economic trade-offs for CO2 impurity specification," *Energy Procedia*, vol. 63, pp. 7379-7388, 2014, doi: https://doi.org/10.1016/j.egypro.2014.11.774.

[3] S. W. Løvseth *et al.*, "CO_2Mix Project: Experimental Determination of Thermo Physical Properties of CO_2-Rich Mixtures," *Energy Proc.*, vol. 37, pp. 2888-2896, // 2013, doi: http://dx.doi.org/10.1016/j.egypro.2013.06.174.

[4] S. W. Løvseth, "ImpreCCS: Lower CCS cost and risk through better CO2 viscosity and thermal conductivity knowledge." [Online]. Available: https://blog.sintef.com/sintefenergy/impreccs-lower-ccs-cost-risk-co2-viscosity-thermal-conductivity/

[5] E. Hendriks *et al.*, "Industrial requirements for thermodynamics and transport properties," *Industrial & engineering chemistry research*, vol. 49, no. 22, pp. 11131-11141, 2010.

[6] S. Peletiri, N. Rahmanian, and I. Mujtaba, "CO2 pipeline design: a review," *Energies*, vol. 11, no. 9, p. 2184, 2018, doi: https://doi.org/10.3390/en11092184.

[7] Y. Tan, W. Nookuea, H. Li, E. Thorin, and J. Yan, "Property impacts on Carbon Capture and Storage (CCS) processes: A review," *Energy Convers. Manage.*, vol. 118, pp. 204-222, 2016.

[8] I. Al-Siyabi, "Effect of impurities on CO_2 stream properties," Heriot-Watt University, 2013.

[9] M. Nazeri, A. Chapoy, R. Burgass, and B. Tohidi, "Viscosity of CO2-rich mixtures from 243 K to 423 K at pressures up to 155 MPa: New experimental viscosity data and modelling," *The Journal of Chemical Thermodynamics*, vol. 118, pp. 100-114, 2018.

[10] S. T. Munkejord, M. Hammer, and S. W. Løvseth, "CO2 transport: Data and models–A review," *Applied Energy*, vol. 169, pp. 499-523, 2016, doi: https://doi.org/10.1016/j.apenergy.2016.01.100.

[11] R. F. Berg, E. F. May, and M. R. Moldover, "Viscosity Ratio Measurements with Capillary Viscometers," (in English), *J. Chem. Eng. Data*, Article vol. 59, no. 1, pp. 116-124, Jan 2014, doi: 10.1021/je400880n.

[12] W. A. Wakeham, "Measurement of the transport properties of fluids," *Experimental thermodynamics*, 1991.

[13] R. F. Berg, E. F. May, and M. R. Moldover, "Viscosity ratio measurements with capillary viscometers," *Journal of Chemical & Engineering Data*, vol. 59, no. 1, pp. 116-124, 2013.

[14] J. B. Mehl, M. L. Huber, and A. H. Harvey, "Ab initio transport coefficients of gaseous hydrogen," *International Journal of Thermophysics*, vol. 31, no. 4, pp. 740-755, 2010, doi: https://doi.org/10.1007/s10765-009-0697-9.

[15] R. F. Berg, "Quartz capillary flow meter for gases," *Review of scientific instruments*, vol. 75, no. 3, pp. 772-779, 2004.

[16] B. Khosravi *et al.*, "A New Facility on Accurate Viscosity and Density Measurements," in *TCCS–11. CO2 Capture, Transport and Storage. Trondheim 22nd–23rd June 2021. Short Papers from the 11th International Trondheim CCS Conference*, 2021: SINTEF Academic Press.

[17] S. F. Westman, H. J. Stang, S. Ø. Størset, H. Rekstad, A. Austegard, and S. W. Løvseth, "Accurate phase equilibrium measurements of CO2 mixtures," *Energy Procedia*, vol. 51, pp. 392-401, 2014.

[18] B. Mangum, "The new International Temperature Scale of 1990 (ITS-90)," *Clinical chemistry*, vol. 35, no. 3, pp. 503-505, 1989, doi: http://dx.doi.org/10.1093/clinchem/35.3.503.